DESIGN OF A COMPACT ION BEAM TRANSPORT SYSTEM FOR THE BELLA ION ACCELERATOR*

Q. Ji†, S. Bulanov, S. Steinke, T. Schenkel, E. H. Esarey, W. P. Leemans
Lawrence Berkeley National Laboratory, Berkeley, CA 94720, USA

Abstract

The Berkeley Lab Laser Accelerator (BELLA) Center hosts a Ti:sapphire CPA laser providing laser pulses at petawatt-level peak power with a repetition rate of 1 Hz. High irradiances of 10^{22} W/cm^2 can be achieved with a short focal length beamline when the laser is focused to a spot of $w_0<5$ μm. Under this condition, theoretical and particle-in-cell (PIC) simulations have shown that protons and helium ions at energies up to several hundred MeV/u can be expected from the interaction between BELLA laser pulses and different targets. Ion beams of high energies, low energy spread and with high controllability and stability have numerous potential applications. A preliminary ion optics design is presented to collect, transport, and focus the ions generated from the laser-driven ion accelerator.

INTRODUCTION

Laser plasma ion acceleration has numerous potential applications such as injectors for conventional accelerators, radiation therapy, studies of radiation damage and single event effect in electronics, as well as fast ignition inertial confinement fusion or material sciences [1-3]. Their unprecedented characteristics, such as short pulse duration, high peak currents and very low transverse emittance, make this technology very attractive.

The accelerating fields generated in ultra-high intensity laser-solid interactions exceed those of conventional accelerators by six orders of magnitude reaching tens of TV/m. Ion bunches with energies of tens of MeV have been generated in such micro-meter scale accelerators. Collimated proton bunches with a continuous, Maxwellian-shape spectrum and energies up to 60 MeV from laser irradiated foils were demonstrated in pioneering experiments more than a decade ago [4]. These triggered an extensive world-wide effort. The maximum proton energy reported did not exceed 67 MeV [5] until the field has experienced major advances recently due to the availability of ultra-high power lasers with focused intensities up to 10^{21} W/cm^2 and laser pulse cleaning techniques that allow a temporal intensity contrast of 14 orders of magnitude [6]. New and very efficient acceleration regimes with nm-thick target foils have been demonstrated with energies up to 100 MeV [7-9]. Mono-energetic proton beams were observed with solid-state lasers and nanofoils [9,10] as well as with CO_2 lasers and gas jet targets [11].

Using a short focal length beam line at BELLA, the PW-class laser facility in operation at LBNL, can offer high peak intensities (>10^{21} W cm^{-2}) and high energy per pulse. As shown in Fig. 1, theoretical and multidimensional computer simulations have shown that several hundred MeV or even GeV protons can be expected from the interaction between BELLA laser pulses with different targets. High ion energies and conversion efficiency, together with ion beam lines to achieve lower divergence and energy spread with high controllability and stability can form the core of a new generation of ion accelerators. Such a high performance laser-driven ion beam system could provide ion beams complimentary to conventional RF accelerators in many novel applications.

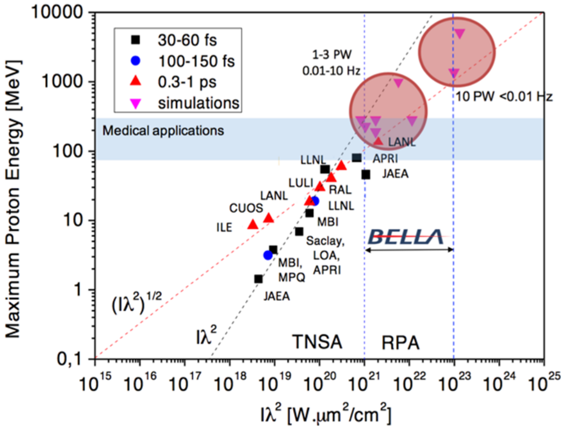

Figure 1: State-of-the-art laser-driven ion accelerator performance and predictions of performance with BELLA [12].

Many applications of using accelerated ions require high energy mono-energetic beams. For example, to make laser-driven ion acceleration system suitable for biomedical applications, especially for radiation therapy related studies [13], the beam should be accelerated up to 250 MeV for protons or ~ 400 MeV/nucleon for carbon ions. An energy spread of 1% or a highly controllable spectrum, with dose on the order of 1-5×10^{10} particles/second have to be demonstrated.

DESIGN AND LAYOUT

Pulsed solenoids, magnetic quadrupoles and RF cavities have been explored by other groups, such as the LIGHT collaboration [14] and ELIMED [15], to transport and shape the ions produced by the laser-driven ion source. The ELIMED transport beam line [15] use permanent magnet quadrupoles (PMQ) placed close to the laser-target interaction point to collect a wide range of ion

---

* Work supported by Laboratory Directed Research and Development (LDRD) funding from Lawrence Berkeley National Laboratory, provided by the Director, Office of Science, of the U. S. Department of Energy under Contract No. DE-AC02-05CH11231.

† Email address: QJi@lbl.gov

energies from 3 to 60 MeV/u, and a dipole energy selection system (ESS) to reduce the beam angular and energy spreads. The beamline was designed to deliver a controllable beam in terms of energy spread varying from 5% up to 20% for the highest energies.

The beam transport and energy selection system described here is designed with a goal of collecting, selecting, and focusing ions at energies over 100 MeV. Instead of PMQs, we adopted a newly developed magnet concept, called a combined-function, alternating-gradient canted cosine theta (AG-CCT) concept, which has been used in compact superconducting gantry design [16]. The magnet consists of multiple CCT quadrupole winding sections placed in sequence on a curve such that the effective current direction is reversed between sections. This produces alternating quadrupole field regions along the length of the bend whose individual integral strengths can be tuned by the location of the current polarity transitions.

The beamline consists of two curved AG-CCT magnets, with combined function of FDFDF quadrupole and dipole structures. The optics is similar to a symmetry-based design of fragment separator [17]. The double mirror symmetry of the system allows that only the specific layout of one-fourth of the system needs to be optimized with the map of the whole system being given by symmetry operations.

Table 1: Properties of the AG-CCT Magnets

	B1	B2
Bore radius (mm)	50	150
Bending radius (m)	1.50	
F Angle (degree)	8.61	
D Angle (degree)	13.76	
F Angle (degree)	15.26	
D Angle (degree)	13.76	
F Angle (degree)	8.61	

The magnitude of the gradient for each of the FDFDF quadrupole sections is the same – only the sign changes. In Table I, the bore radius, bending radius, and angular lengths for the magnets are given. The general approach of a sharp cut-off fringe field (SCOFF) model of the magnets is used to arrive at an initial beamline design. For different ion energies, the gradient of the magnets can be tuned to transport the ions of interested. The quadrupole gradient and dipole magnet field required for ions at various of energies are listed in Table 2.

COSY INFINITY code [18] was used to calculate the first order beam envelope corresponding to an initial beam of 1 mm diameter, half diverging angle of 40 mrad, and ± 12% energy dispersion going through two AG-CCT combined function magnets. The rays are shown in Fig. 2.

The beamline allows ions with a large energy dispersion to be transported, and a slit can be placed in the centre of the beamline to select a specific energy of interest with small energy spread to be further focused to the target.

Table 2: Quadrupole Gradients and Dipole Fields for Ions at Various Energies

Beam Energy (MeV/u)	Quadrupole gradient (T/m)	Dipole field (T)
200	25.4	1.4
150	21.7	1.2
100	17.5	0.96
50	12.3	0.67
25	8.6	0.47
10	5.4	0.3

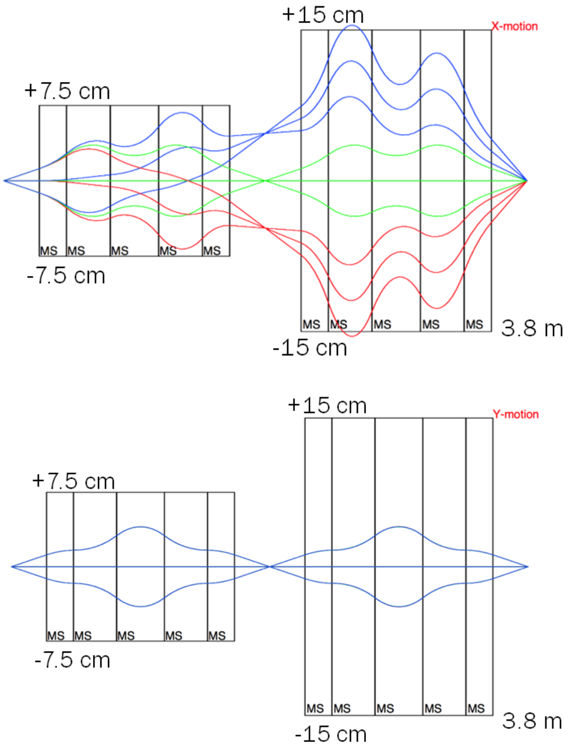

Figure 2: First order horizontal beam envelope corresponding to an initial beam of ± 1 mm, ± 40 mrad, and ± 12% energy dispersion going through two AG-CCT combined function magnets. The aperture size of each magnet is 15 cm and 30 cm respectively. (top) x-axis, and (bottom) y-axis.

The diverging angles of the initial ion beam entering the beamline, show in Fig. 3 (top), were calculated based on the momentum and energy distribution of protons in the Directed Coulomb Explosion (DCE) regime of acceleration for a 0.5 PW laser pulse and a double-layer foil, modelled in 2D using REMP codes [19]. The beam is then tracked through the transfer map of the system. The ion beam distribution (with energy dispersion of ± 12%) reaching the target after going through the AG-CCT magnets is plotted in Fig. 3 (bottom). Higher order effect due to the combination of the magnets need to be taken into account in the future.

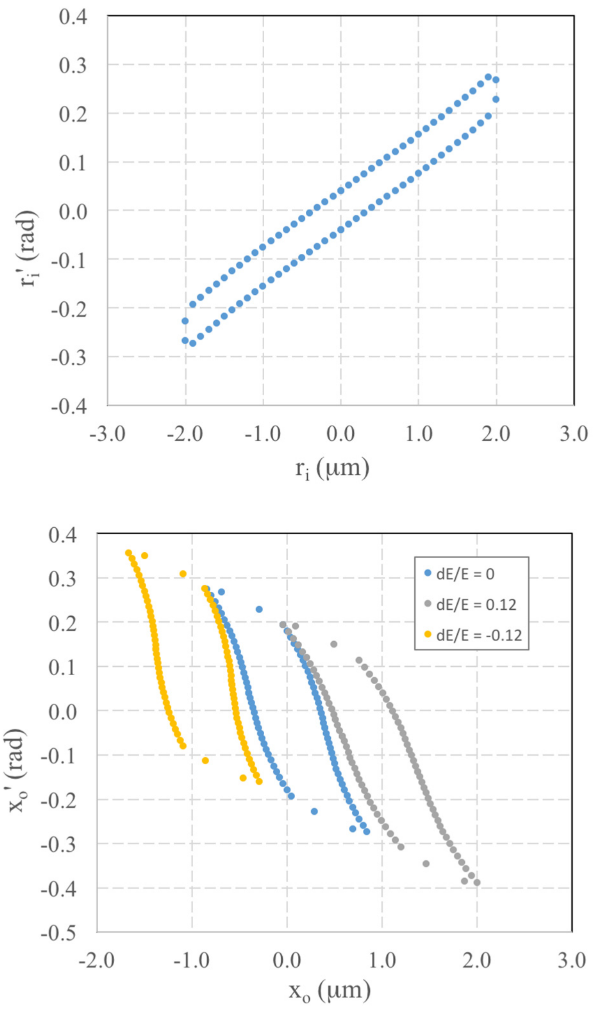

Figure 3: (top) The emittance plot of the initial beam based on the REMP 2D simulation of the laser-target interaction; (bottom) The emittance plot of the ion beam (with energy dispersion of ± 12%) reaching the target after going through the AG-CCT magnets.

It is a challenge to reduce the beam energy spread below 1% without losing too many particles. As shown in Fig. 4, a discharge capillary as an active plasma lens [20] can be placed a couple of centimetres away from the laser target to capture ions at large diverging angle. The energy spread of the ions can be further reduced by going through an RF cavity [14, 21] acting as a phase rotator. When the phase of the RF field is properly tuned the faster ions arriving earlier at the RF cavity are decelerated while the slower ions arriving later are accelerated, resulting in a significantly reduction in the energy spectral band.

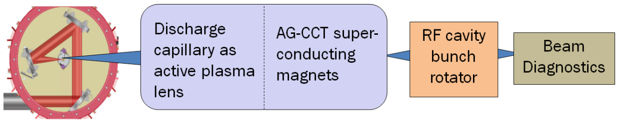

Figure 4: Proposed beamline including the laser-target chamber, active plasma lens, AG-CCT combined function magnets, RF cavity bunch rotator.

SUMMARY

A preliminary design of a compact beam transport and energy selection system using combined function AG-CCT magnets is presented. As opposed to PMQ, this design allows, by varying the magnetic field, to transport ions at a large energy range, varying from 10 MeV to 200 MeV, with initial beam diverging angle less than ± 40 mrad, and energy dispersion less than ± 12%. More simulations are needed to add components such as an active plasma lens, which can be located close to the laser target to capture more ions, and an RF cavity, which can result in a significant narrowing of the energy spectral band.

ACKNOWLEDGMENT

The authors would like to thank Dr. Weishi Wan for his help with COSY Infinity code and discussions on the AG-CCT beamline design.

REFERENCES

[1] G. Mourou et al, Rev. Mod. Phys 78, 309, 2006.

[2] H. Daido et al, Rep. Prog. Phys. 75, 056401, (2012.

[3] A. Macchi et al, Rev. Mod. Phys. 85, 751, 2013.

[4] R. A. Snavely et al, Phys. Rev. Lett. 85, 2945-2948, 2000.

[5] K. Flippo et al, Journal of Physics: Conference Series 244, 022033, 2010.

[6] K. Ogura et al, Optics Letters 37, 2868, 2012.

[7] I. J. Kim et al, Phys. Rev. Lett. 111, 165003, 2013.

[8] D. Jung et al, Physics of plasmas, 20, 083103, 2013.

[9] B. M. Hegelich et al, arXiv:1310.8650.

[10] A. Henig et al, Phys. Rev. Lett. 103, 245003, 2009.

[11] D. Haberberger et al, Nature Phys. 8, 95, 2012.

[12] S. S. Bulanov et al, Physics of plasmas, 23, 056703, 2016.

[13] S. V. Bulanov and V. S. Khoroshkov, Plasma Phys. Rep. 28, 453, 2002).

[14] S. Busold et al, Nucl. Instru. Meth. Phys. Res. A, 740, 94(2014); Phys. Rev. STAB 17, 031302, 2014).

[15] F. Romano et al, Nucl. Instru. Meth. Phys. Res. A, 2016, http://dx.doi.org/10.1016/j.nima.2016.01.064

[16] W. Wan et al, Phys. Rev. STAB 18, 103501, 2015.

[17] B. Erdelyi et al, Phys. Rev. STAB 10, 064002, 2007.

[18] M. Berz and K. Makino, COSY Infinity program, http://www.bt.pa.msu.edu/index_cosy.htm

[19] O. Rubel, B. Loring, J.-L. Vay, D. P. Grote, R. Lehe, S. S. Bulanov, H. Vincenti, and E. W. Bethel, submitted to IEEE CG&A, in press.

[20] J. van Tilborg et al, Phys. Rev. Lett. 115, 184802, 2015.

[21] S. Nakamura et al, Japan. J. Appl. Phys. 46, L717, 2007.